



Article

Co-Treatment with Phlorotannin and Extracellular Vesicles from *Ecklonia cava* Inhibits UV-Induced Melanogenesis

Kyung-A Byun ^{1,2,3,†}, Youngjin Park ^{4,†}, Seyeon Oh ³, Sosorburam Batsukh ^{1,3}, Kuk Hui Son ^{5,*} and Kyunghee Byun ^{1,3,6,*}

¹ Department of Anatomy & Cell Biology, College of Medicine, Gachon University, Incheon 21936, Republic of Korea

² LIBON Inc., Incheon 22006, Republic of Korea

³ Functional Cellular Networks Laboratory, Lee Gil Ya Cancer and Diabetes Institute, Gachon University, Incheon 21999, Republic of Korea

⁴ OBLIV CLINIC, Incheon 21998, Republic of Korea

⁵ Department of Thoracic and Cardiovascular Surgery, Gachon University Gil Medical Center, Gachon University, Incheon 21565, Republic of Korea

⁶ Department of Health Sciences and Technology, Gachon Advanced Institute for Health & Sciences and Technology (GAIHST), Gachon University, Incheon 21999, Republic of Korea

* Correspondence: dr632@gachon.ac.kr (K.H.S.); khbyun1@gachon.ac.kr (K.B.); Tel.: +82-32-460-3666 (K.H.S.); +82-32-899-6511 (K.B.)

† These authors contributed equally to this work.

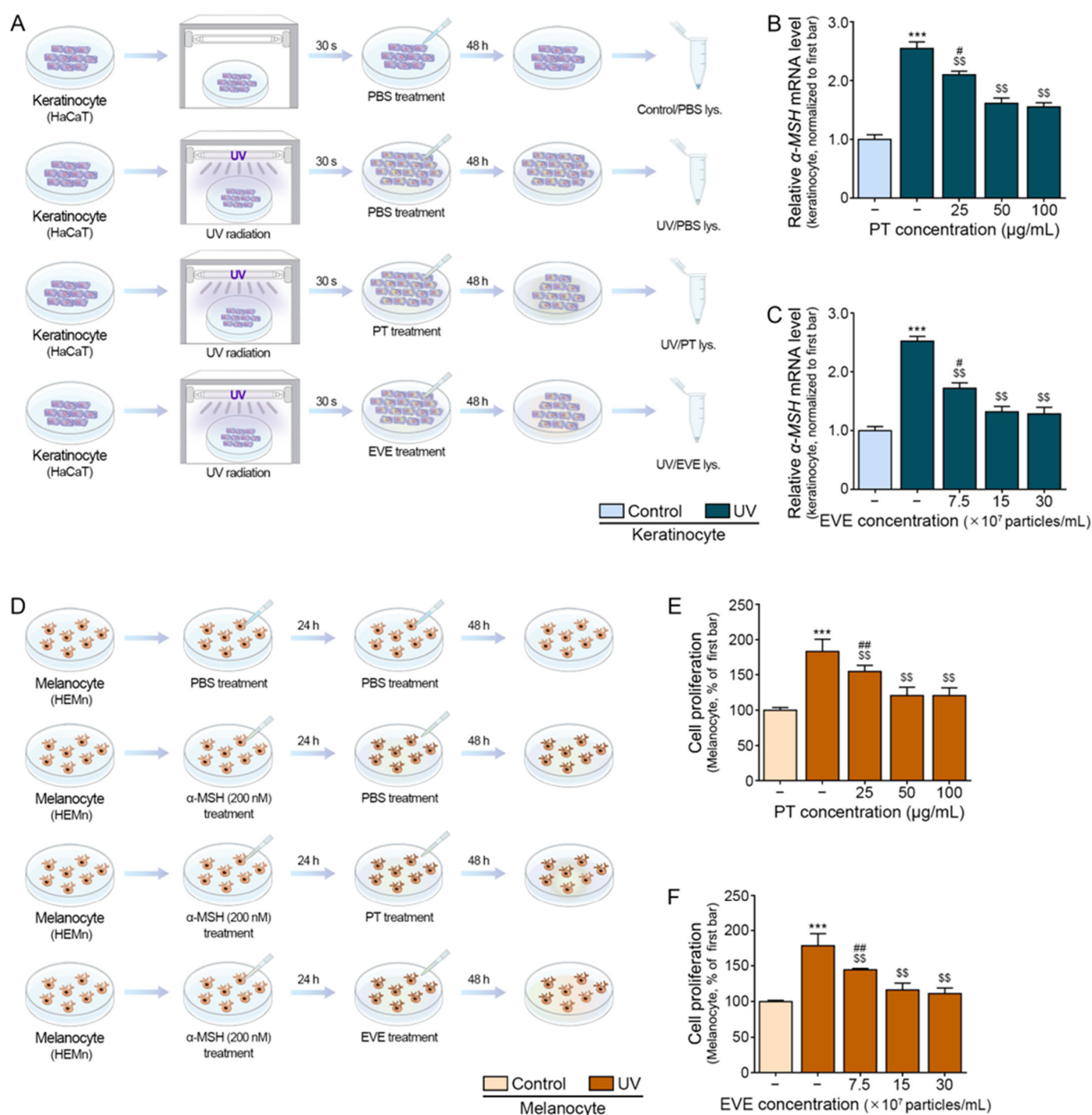


Figure S1. Optimization of PT and EVE concentrations *in vitro*. **(A)** Schematic diagram of the treatment of UV-exposed keratinocytes with PT or EVE. **(B,C)** The mRNA levels of α -MSH in UV-exposed keratinocytes following PT **(B)** or EVE **(C)** treatment were measured by qRT-PCR. **(D)** Schematic diagram of the treatment of melanocyte with PT or EVE. **(E,F)** Cell proliferation was assessed in melanocytes following PT **(E)** or EVE **(F)** treatment by CCK-8 assay. Data are presented as the mean \pm SD of three independent experiments. ***, $p < 0.001$, first bar vs. second bar; \$\$, $p < 0.01$, second bar vs. third, fourth, fifth bar; #, $p < 0.05$ and ##, $p < 0.01$, fifth bar vs. third, fourth bar (Mann–Whitney U test). α -MSH, α -melanocyte-stimulating hormone; EVE, extracellular vesicles from *E. cava.*; PBS, phosphate-buffered saline; PT, phlorotannin; qRT-PCR, quantitative reverse-transcription polymerase chain reaction; SD, standard deviation; UV, ultraviolet.

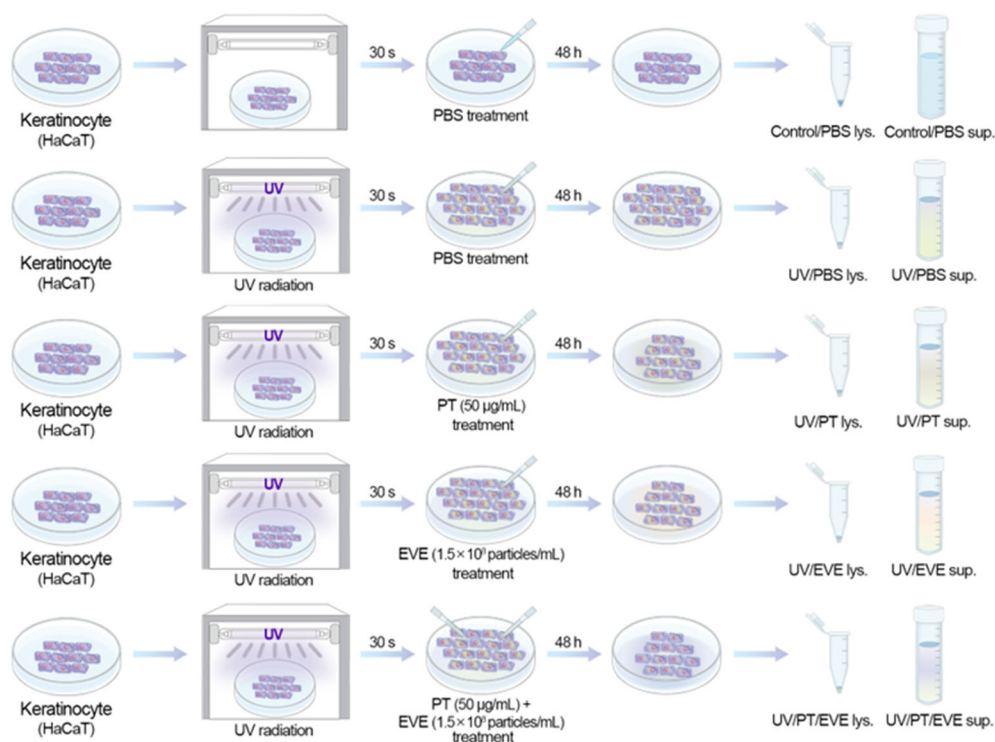


Figure S2. Schematic of keratinocytes with UV-induced pigmentation for the evaluation of PT and EVE. EVE, extracellular vesicles from *E. cava*; lys, lysate; PBS, phosphate-buffered saline; PT, phlorotannin; sup, supernatant; UV, ultraviolet.

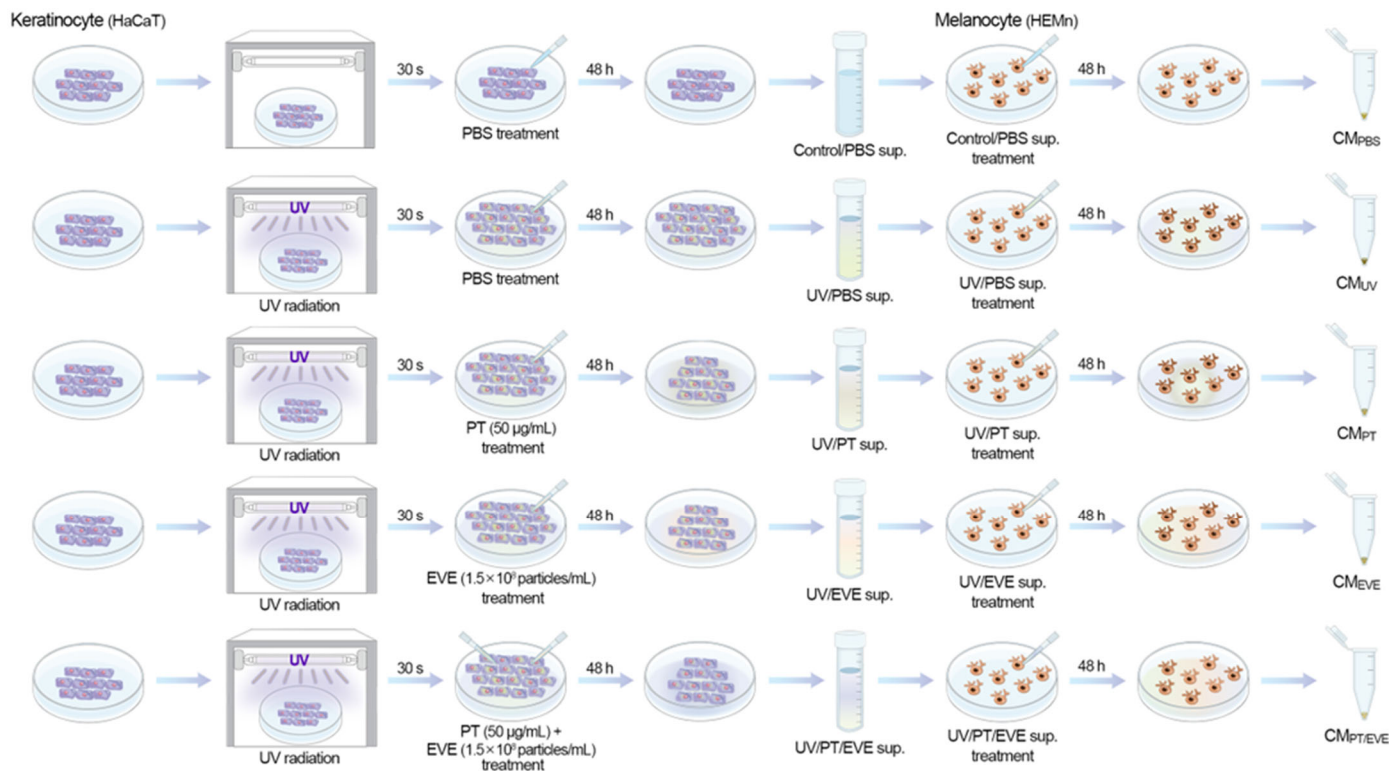


Figure S3. Schematic of melanocytes affected by keratinocytes with UV-induced pigmentation for the evaluation of PT and EVE. CM, conditioned media from keratinocyte; EVE, extracellular vesicles from *E. cava*; PBS, phosphate-buffered saline; PT, phlorotannin; sup, supernatant; UV, ultraviolet.

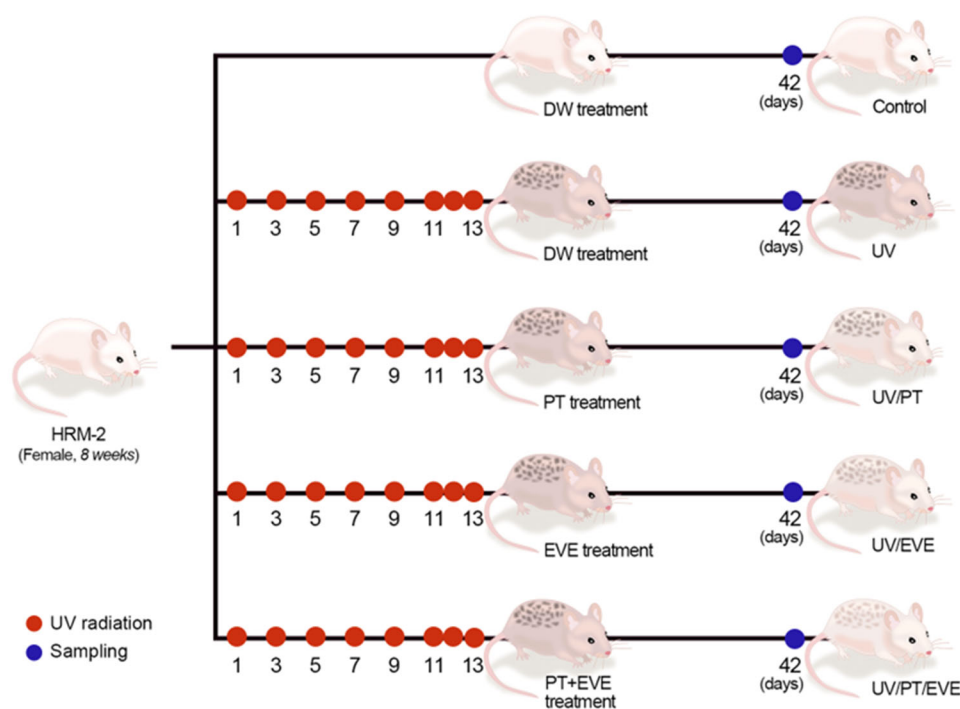


Figure S4. Schematic of mice with UV-induced pigmentation for the evaluation of PT and EVE. On 2 weeks after UV radiation starting, PBS, PT (concentration of 1 mg/mL), EVE (concentration of 3.0×10^{10} particles/mL), or mixture of PT and EVE (each of concentration of 1 mg/mL and 3.0×10^{10} particles/mL) was administered into animal skin with micro needling system. Total injection volume of all solution was 200 μ L. After 28 days of injection, animal skin was harvested. DW, distilled water; EVE, extracellular vesicles from *E. cava*; PT, phlorotannin; UV, ultraviolet.

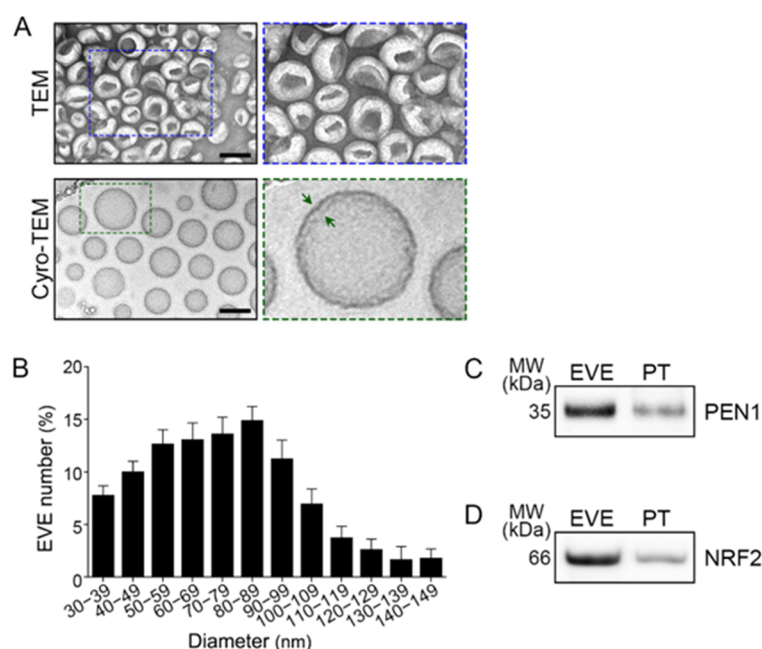


Figure S5. (A) TEM image of EVE and confirmation of surface marker and NRF2 expression in EVE and PT. Blue dotted lines indicate a magnified image of negative staining. Green dotted lines represent a magnified image of cryo-TEM, and the green arrows show a lipid bilayer membrane of a vesicle. Scale bar= 100 nm. (B) Quantitative assessment of EVE diameter based on TEM images. (C,D) Western blot analysis of plant EV markers PEN1 (C) and NRF2 (D) in PT and EVE. EVE, extracellular vesicles from *E. cava*; MW, molecular weight; NRF2, nuclear factor erythroid-2-related factor 2; PEN1, penetration 1; PT, phlorotannin; TEM, transmission electron microscopy.

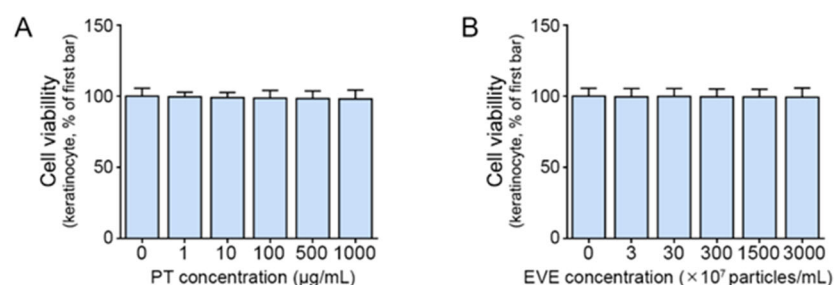


Figure S6. *In vitro* cytotoxic effects of PT and EVE treatments. (A,B) The cell viability of keratinocytes following PT (A) or EVE (B) treatment was measured. Data are presented as the mean \pm SD of three independent experiments. EVE, extracellular vesicles from *E. cava*; PT, phlorotannin; SD, standard deviation.

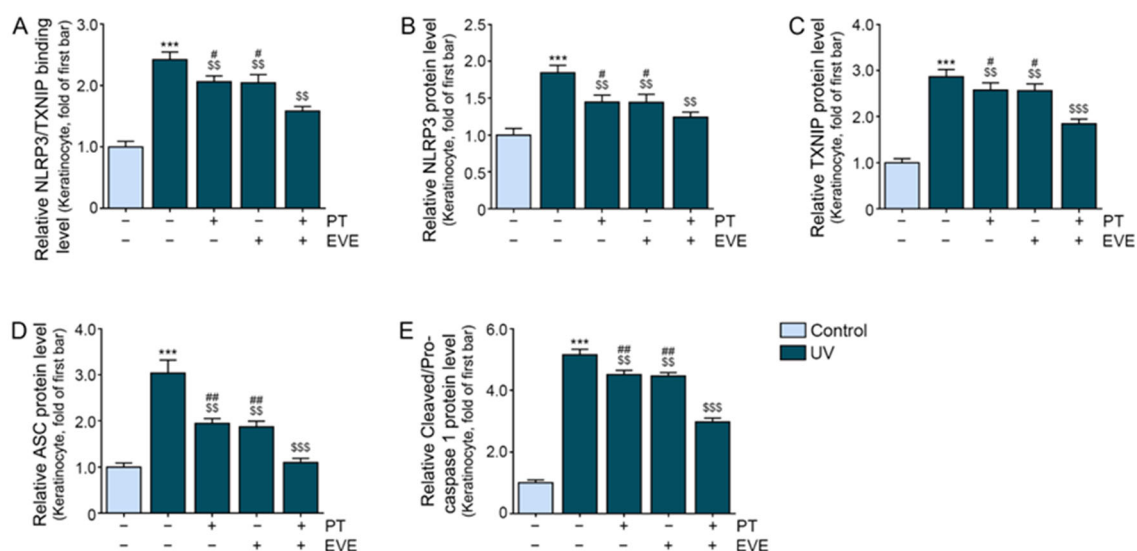


Figure S7. Regulation of NLRP3 inflammasome by PT and EVE treatments in UV-exposed keratinocytes. (A–C) Quantitative assessment of Western blot data presented in Figure 2A. (D,E) Quantitative assessment of Western blot data presented in Figure 2B. Data are presented as the mean \pm SD of three independent experiments. ***, $p < 0.001$, first bar vs. second bar; \$\$, $p < 0.01$ and \$\$\$, $p < 0.001$, second bar vs. third, fourth, fifth bar; #, $p < 0.05$ and ##, $p < 0.01$, fifth bar vs. third, fourth bar (Mann–Whitney U test). ASC, apoptosis-associated speck-like protein containing a caspase recruitment domain; EVE, extracellular vesicles from *E. cava*; NLRP3, nucleotide-binding oligomerization domain-like receptor family pyrin domain containing 3; PT, phlorotannin; SD, standard deviation; TXNIP, Thioredoxin-interacting protein; UV, ultraviolet.

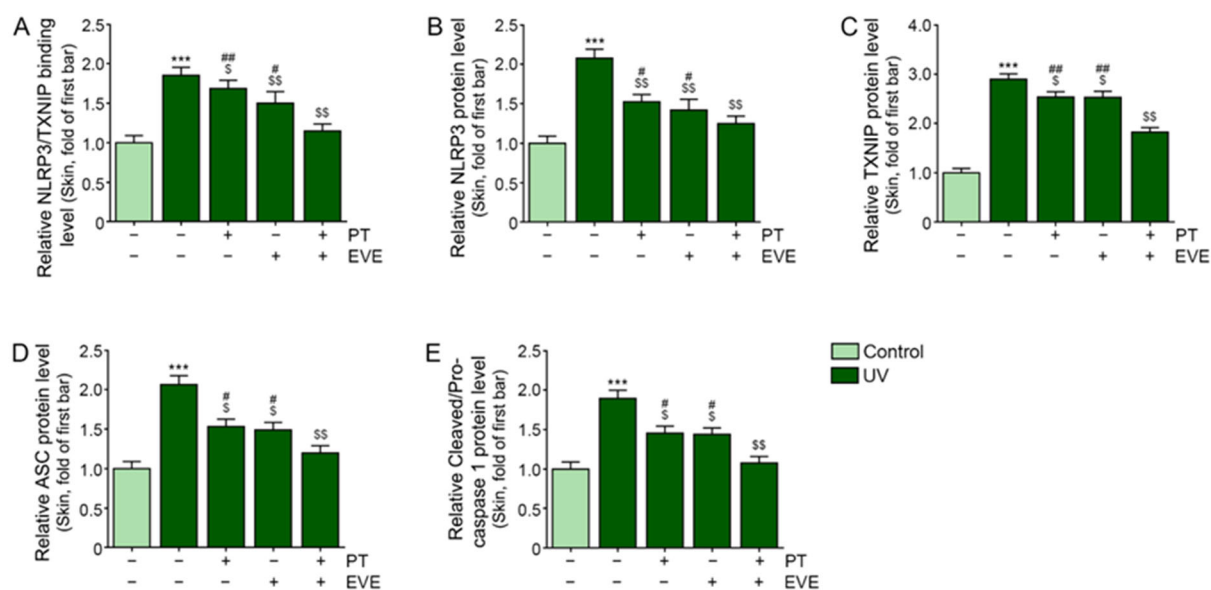


Figure S8. Regulation of NLRP3 inflammasome by PT and EVE treatments in UV-exposed animal skin. (A–C) Quantitative assessment of Western blot data presented in Figure 2C. (D,E) Quantitative assessment of Western blot data presented in Figure 2D. Data are presented as the mean \pm SD of three independent experiments. ***, $p < 0.001$, first bar vs. second bar; \$, $p < 0.05$ and \$\$, $p < 0.01$, second bar vs. third, fourth, fifth bar; #, $p < 0.05$ and ##, $p < 0.01$, fifth bar vs. third, fourth bar (Mann–Whitney U test). ASC, apoptosis-associated speck-like protein containing a caspase recruitment domain; EVE, extracellular vesicles from *E. cava*; NLRP3, nucleotide-binding oligomerization domain-like receptor family pyrin domain containing 3; PT, phlorotannin; SD, standard deviation; TXNIP, Thioredoxin-interacting protein; UV, ultraviolet.

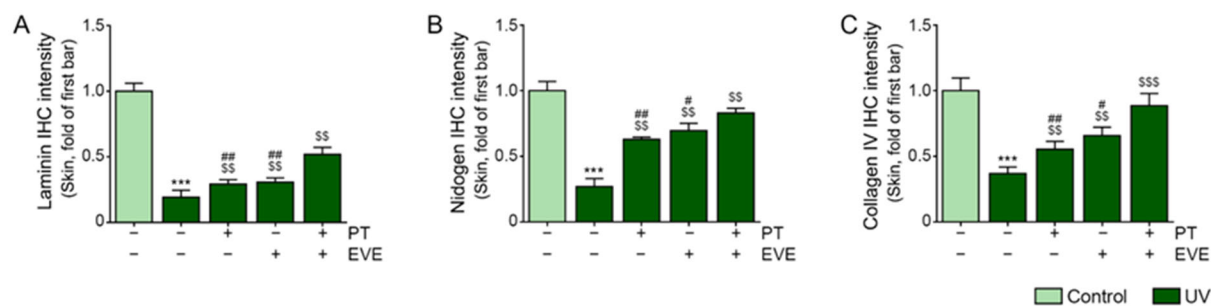


Figure S9. Regulation of BM components by PT and EVE in UV-exposed animal skin. (A–C) Quantitative assessment of IHC presented in Figure 3J. Data are presented as the mean \pm SD of three independent experiments. ***, $p < 0.001$, first bar vs. second bar; \$\$, $p < 0.01$ and \$\$\$, $p < 0.001$, second bar vs. third, fourth, fifth bar; #, $p < 0.05$ and ##, $p < 0.01$, fifth bar vs. third, fourth bar (Mann–Whitney U test). BM, basement membrane; EVE, extracellular vesicles from *E. cava*; IHC, immunohistochemistry; PT, phlorotannin; SD, standard deviation; UV, ultraviolet.

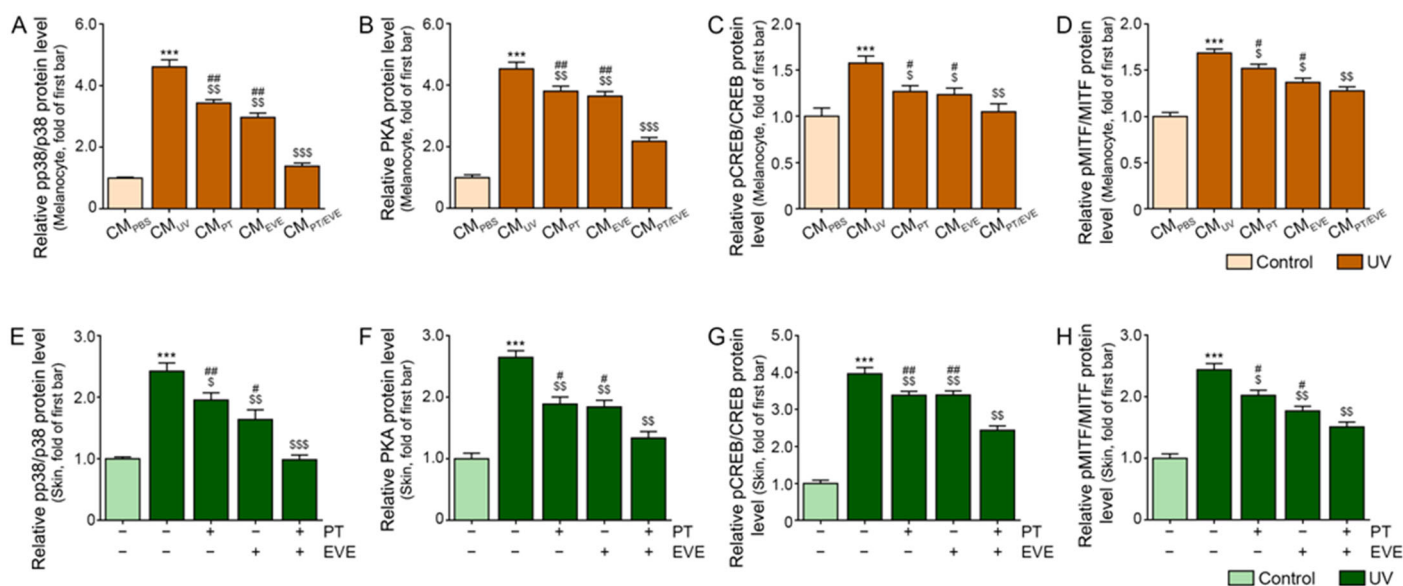


Figure S10. Regulation of melanogenesis pathway signals by PT and EVE in melanocytes and UV-exposed animal skin. (A–H) Quantitative assessment of Western blot data presented in Figure 4A (A–D) and Figure 4E (E–H). Data are presented as the mean ± SD of three independent experiments. ***, $p < 0.001$, first bar vs. second bar; \$, $p < 0.05$, \$\$, $p < 0.01$, \$\$\$, $p < 0.001$, second bar vs. third, fourth, fifth bar; #, $p < 0.05$ and ##, $p < 0.01$, fifth bar vs. third, fourth bar (Mann–Whitney U test). CM, conditioned media; CREB, cAMP response element binding protein; EVE, extracellular vesicles from *E. cava*; MITF, microphthalmia-associated transcription factor; p, phosphorylated; PBS, phosphate-buffered saline; PKA, protein kinase A; pCREB, phosphorylated CREB; pMITF, phosphorylated MITF; PT, phlorotannin; pp38, phosphorylated p38; SD, standard deviation; UV, ultraviolet.

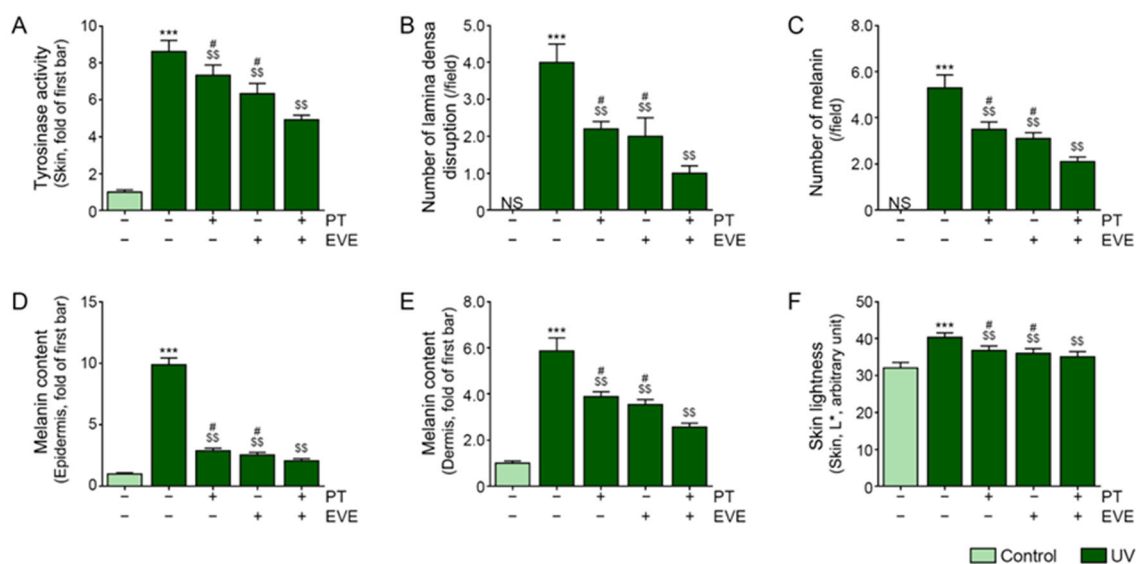


Figure S11. Regulation of melanin accumulation by PT and EVE treatments in UV-exposed animal skin. (A) The tyrosinase activity in UV-exposed mouse skin following PT and EVE treatment was measured. (B,C) Quantitative assessment of TEM images presented in Figure 5A. (D,E) Quantitative assessment of Fontana Masson staining in the epidermis and dermis of mouse skin presented in Figure 5B. (F) Quantitative assessment of skin lightness measured using a CR-10 color reader presented in Figure 5C. Data are presented as the mean ± SD of three independent experiments. ***, $p < 0.001$, first bar vs. second bar; \$\$, $p < 0.01$, second bar vs. third, fourth, fifth bar; #, $p < 0.05$, fifth bar vs. third, fourth bar (Mann–Whitney U test). EVE, extracellular vesicles from *E. cava*; NS, non-signals; PT, phlorotannin; SD, standard deviation; TEM, transmission electron microscopy; UV, ultraviolet.

Table S1. Concentration analysis of EVE used in this study.

	Initial <i>E. cava</i> material	12 g
NTA	Diluent	2000
	dilution concentration	$1.82 \pm 0.15 \times 10^8$ particles/mL
	Total concentration	$3.64 \pm 0.29 \times 10^{11}$ particles/mL
	Concentration per 1 g of <i>E. cava</i>	$3.03 \pm 0.24 \times 10^{10}$ particles/mL
BCA	Concentration	11.8 mg/mL
	Concentration per 1 g of <i>E. cava</i>	0.98 mg/mL

BCA, bicinchoninic acid assay; EVE, extracellular vesicles from *E. cava*; NTA; nanoparticle-tracking analysis.

Table S2. List of primers for quantitative reverse–transcription polymerase chain reaction.

Accession Number	Gene (Organism)		Primer Sequences
NM_001101.5	<i>ACTB (human)</i>	Forward	5'-CTC GCC TTT GCC GAT CC-3'
		Reverse	5'-TCT CCA TGT CGT CCC AGT TG-3'
NM_003998.4	<i>NF-κB (human)</i>	Forward	5'-ACC TAG CTG CCA AAG AAG GAC-3'
		Reverse	5'-TGG GGT GGT CAA GAA GTA GTG-3'
NM_004530.6	<i>MMP2 (human)</i>	Forward	5'-CAC TTT CCT GGG CAA CAA ATA-3'
		Reverse	5'-CTT GCG GTC ATC ATC GTA GTT-3'
NM_004994.3	<i>MMP9 (human)</i>	Forward	5'-AAA GCC TAT TTC TGC CAG GAC-3'
		Reverse	5'-TCA TAG GTC ACG TAG CCC ACT-3'
NM_000372.5	<i>TYR (human)</i>	Forward	5'-TGT TTT GTA CTG CCT GCT GTG-3'
		Reverse	5'-AGC ATT CCT TCT CCA TCA GGT-3'
NM_000550.3	<i>TRP1 (human)</i>	Forward	5'-GTG CCA CTG TTG AGG CTT TG-3'
		Reverse	5'-ATG GGG ATA CTG AGG GCT GT-3'
NM_001922.5	<i>TRP2 (human)</i>	Forward	5'-AAA GCC TGA CTT AAC GGG GG-3'
		Reverse	5'-GGA TTT TGC AGC CCA AGC AA-3'
NM_000939.4	<i>α-MSH (human)</i>	Forward	5'-GTT TCA TGA CCT CCG AGA AGA G-3'
		Reverse	5'-CTT GTA GGC GTT CTT GAT GAT G-3'
NM_007393.5	<i>Actb (mouse)</i>	Forward	5'-CCG TAA AGA CCT CTA TGC CAA C-3'
		Reverse	5'-GCA GTA ATC TCC TTC TGC ATC C-3'
NM_008689.3	<i>Nf-κb (mouse)</i>	Forward	5'-CAG TGG TGT GGA GAC ATC CTT-3'
		Reverse	5'-TCA GAG ATA GCA GTG GGC TGT-3'
NM_008610.3	<i>Mmp2 (mouse)</i>	Forward	5'-GAT GAT GAC CGG AAG TGG GG-3'
		Reverse	5'-ATG AAG ATG ATA GGG CCC GTG-3'
NM_013599.5	<i>Mmp9 (mouse)</i>	Forward	5'-GGG TCT AGG CCC AGA GGT AA-3'
		Reverse	5'- TAA CGC CCA GTA GAG AGC CT-3'
NM_011661.6	<i>Tyr (mouse)</i>	Forward	5'-CAG CAT CCT TCT TCT CCT CCT-3'
		Reverse	5'-GTT CCA TCG CAT AAA ACC TGA-3'
NM_031202.3	<i>Trp1 (mouse)</i>	Forward	5'-AGG GTG GAC CAA TCA GGA GA-3'
		Reverse	5'-CCG CAT CAG TGA AAG TGT GC-3'
NM_010024.3	<i>Trp2 (mouse)</i>	Forward	5'-CCT GAA TGG GAC CAA TGC CT-3'
		Reverse	5'-GAA AAG CCA GCA ACC CCA AG-3'
NM_201394.2	<i>Plectin (mouse)</i>	Forward	5'-GCT TTC GAT CAC TGA GTT TGC-3'
		Reverse	5'-ACT GAT GGG GTA GGA GGA AGA-3'
NM_001276764.1	<i>Bp230 (mouse)</i>	Forward	5'-CAC CGC GAG CAG ATA ATA GAG-3'
		Reverse	5'-GAG CAG GTT CTT GAT GAG CAC-3'
NM_009842.3	<i>Cd151 (mouse)</i>	Forward	5'-CAT TAG TCT GCT GGC CTC AAG-3'
		Reverse	5'-GTC ACC ATG ACA ACA ACA CCA-3'

Table S3. List of antibodies for Western blot (WB), Enzyme-linked immunosorbent assay (ELISA), and Immunohistochemistry (IHC).

Antibody	Company	Catalog No.	Dilution Rate		
			WB	ELISA	IHC
HO-1	Abcam	ab13248	1:500		
β -actin	Cell Signaling	4967	1:1,000		
8-OHdG	GeneTex	GTX41980		1:500	
NLRP3	BosterBio	M00034	1:500		
TXNIP	Cell Signaling	14715	1:1,000		
ASC	Santa Cruz	sc-271054	1:500		
Cleaved-caspase 1	Cell Signaling	89332	1:1,000		
Pro-caspase 1	Santa Cruz	sc-392736	1:500		
IL-18	Invitrogen	PA5-79481		1:500	
Laminin	Novus Biological	NB300-144			1:200
Nidogen	Santa Cruz	sc-47773			1:50
Collagen IV	Invitrogen	PA1-28534			1:100
p38	Cell Signaling	9212	1:1,000		
pp38	Cell Signaling	4511	1:1,000		
PKA	Santa Cruz	sc-390548	1:500		
CREB	Sigma-Aldrich	C8977	1:1,000		
pCREB	Cell Signaling	9198	1:1,000		
MITF	LSBIO	LS-C117668	1:500		
pMITF	BT LAB	BT-AP11347	1:500		